7th April 2015

Microwire Chronoamperometric Determination of Concentration, Diffusivity, and Salinity for Simultaneous Oxygen and Proton Reduction

James Weber [1], Andrew J. Wain [2], and Frank Marken *[1]

[1] *Department of Chemistry, University of Bath, Claverton Down, Bath BA2 7AY, UK*
[2] *National Physical Laboratory, Teddington, United Kingdom, TW11 0LW, UK*

To be submitted to Electroanalysis

Proofs to F. Marken

Email F.Marken@bath.ac.uk

Abstract

A microwire chronoamperometric method is reported employing a 25 μm diameter platinum microwire for multi-parameter electroanalysis with digital simulation-based evaluation (employing DigiElch 4.F). Concentration and diffusion coefficient data are obtained for the reduction of oxygen and for the reduction of protons individually and simultaneously in saline (0.1 M to 4.0 M NaCl) electrolyte media. The diffusion coefficient and concentration data for oxygen allows salinity levels to be estimated. The microwire chronoamperometry method offers versatility and precision due to (i) a slow approach to steady state (when compared to microdisc methods) and (ii) insignificant viscosity effects (when compared to hydrodynamic methods).

Keywords: microwire electrode, voltammetry, brine, hydrogen, salt, corrosion, pH, sensor.

Graphical abstract

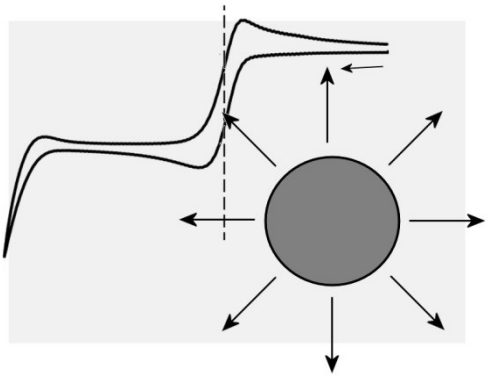

1. Introduction

Microcylindrical electrodes [1,2,3], also referred to as microwire electrodes, have been initially developed into electroanalytical devices in pioneering work by Aoki *et al.* [4]. Later these types of electrodes found a wider range of applications from sensors for foodborne pathogens [5] or anti-oxidants [6] to hydrogen peroxide and glucose determination [7], as well as for the electroanalytical detection of drugs [8] and trace metal ions or sulphide in seawater [9,10,11]. Recently "nano-impact" experiments have been reported for the detection of single nanoaprticles at micro-wire electrodes [12]. Gründler and coworkers [13] have also used microwire electrodes extensively in fast temperature pulse or "hot-wire voltammetry" for analytical applications [14]. The relative ease of fabricating microwire electrodes and modelling data from electrochemical measurements provide important benefits in comparison to other geometries such as more conventional planar disks [15].

Over recent years, powerful methods for the quantitative analysis of chronoamperometric data from microwire electrodes have been developed [16] to allow information from potential step transients to be extracted. Generally, this type of transient data is composed of two regimes. In the early stages of the transient, planar diffusion dominates and so the measured current will closely follow the Cottrell equation [17] (equation 1):

$$I(t) = nFA\sqrt{D}c \times \frac{1}{\sqrt{\pi t}} \qquad (1)$$

In this equation the current I is given by n, the number of electrons transferred per molecule diffusing to the electrode surface, F, the Faraday constant, $A=2\pi rl$, the electrode area with r the radius and l the length, D, the diffusion coefficient, c, the bulk concentration, and t, the time. At longer timescales additional current due to curvature in the diffusion field around the microwire is observed, leading to a quasi-steady state cylindrical diffusion profile. An approximate analytical expression [18] (equation 2) has been reported that captures the current-time response under this regime:

$$I(t) = nFlDc \times \left(\frac{\pi e^{-\frac{2}{5}\sqrt{\pi \frac{Dt}{16r^2}}}}{4\sqrt{\pi \frac{Dt}{16r^2}}} + \frac{\pi}{\ln\left[\sqrt{64e^{-0.5772\frac{Dt}{16r^2}} + e^{\frac{5}{3}}}\right]} \right) \quad (2)$$

Whilst equations 1 and 2 are valid to a good approximation at short and long times respectively, numerical methods are more suitable at intermediate timescales and for more complex cases including such as simultaneous redox processes. Commercial simulation packages such as DigiElch [19,20] now enable such current transients to be computed over the full range of times by numerically integrating the diffusion equation under a user-defined set of boundary conditions. This program iterates a single variable whilst outputting the calculated standard deviation from the input data, thus enabling optimal values for experimental parameters such as electrode length, concentration, diffusion coefficients etc., to be determined manually without the need to resort to multi-parameter non-linear fitting.

The numerical simulation of chronoamperometric data provides a useful means to highlight the benefits of the microwire geometry as compared to more conventional microdisc electrodes. Figure 1 shows transient data generated using the DigiElch package for microdisc (A) and microwire (B) electrodes of identical diameter (25 μm), with D given the nominal value of 10^{-9} m^2s^{-1}. Simulated curves exhibit initially a rapid decay followed by a more gentle decay consistent with the expected transition from planar diffusion (following equation [21]) towards a (quasi) steady state regime in which microdisc [22] and microwire [18] transient behaviour is observed (see line (i)). The transition in diffusion regime occurs when the diffusion layer thickness (δ) approximately equals the electrode radius (= 12.5 μm), and is parameterised by the transition time, $\tau = \delta^2/D$ = 156 ms.

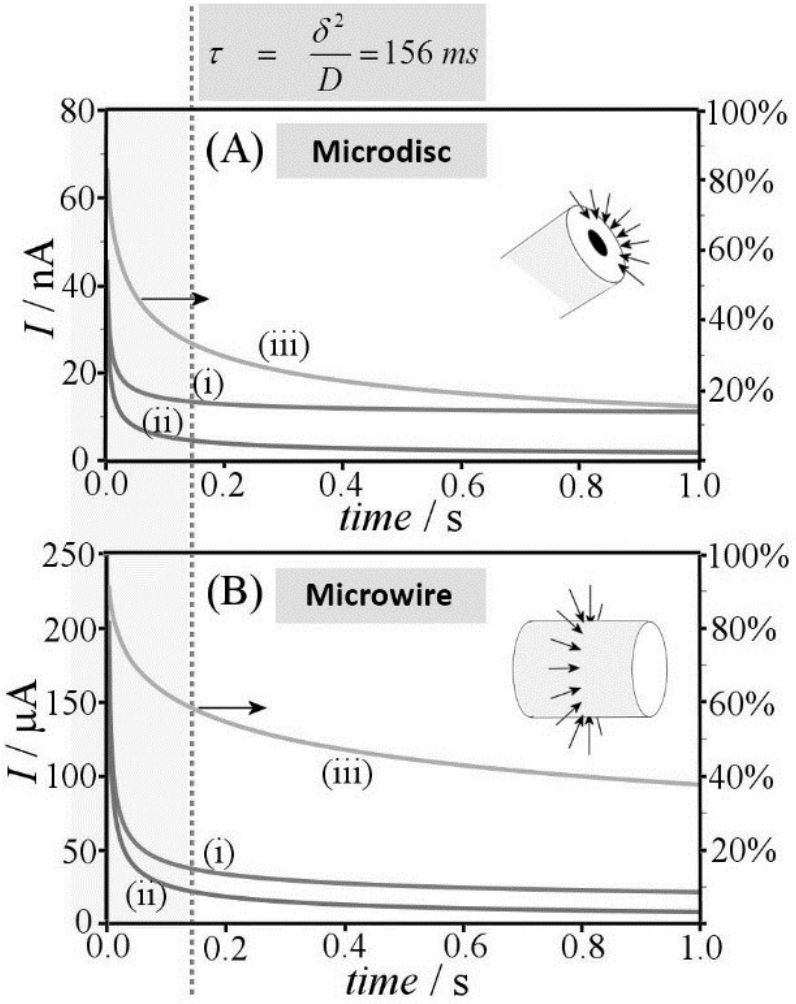

Figure 1. Simulated decay (calculated with DigiElch 4.F) of chronoamperometry current for (A) a 25 μm diameter disk and (B) a 25 μm diameter microwire with (i) the current trace, (ii) the Cottrell only current trace assuming a planar electrode of the same area, and (iii) the percentage of "Cottrellness" (= 100 × $I_{Cottrell}/I_{Total}$) when going from planar transient towards steady state current with a transition point τ.

Mathematically, the simultaneous determination of concentration and diffusion coefficient values from such chronoamperometric data is possible only because of the switch in diffusion regime. Data in the time domain with purely planar diffusion (early) and that in the time domain with (quasi) steady state diffusion (late) contribute only little to the information content of the transient, so analysis of data from the transition region is necessary for *c* and *D* to be determined simultaneously [23,24]. The degree of

useful information contained in the transient at a given time can be assessed by considering how the current compares to the "Cottrell only" response, plotted as line (ii) in Figure 1, since this represents the hypothetical situation in which no transition to (quasi) steady state behaviour occurs. Line (iii) in Figure 1 plots the Cottrell only current as a fraction of the total current from which it is clear that this level of "Cottrellness" (= $100 \times I_{Cottrell}/I_{Total}$) is generally much higher across the length of the transient for the microwire than the microdisc. As a result, the microwire provides a more informative current response over a longer period of time which should be advantageous in the reliable evaluation of c, D, and other parameters using numerical fitting methods.

The focus of the present paper is the electroanalytical challenge of the determination of concentration and diffusion coefficient data in highly saline media. It is shown that the concentration of two important redox systems can be determined simultaneously with the salinity. Measurements in concentrated salt media are notoriously difficult due to salt affecting heterogeneous kinetics [25] and mobility of ions [26,27] as well as electrode performance. Furthermore, significant solubility effects can be observed, such as a decrease in dissolved oxygen concentration (salting out) with increasing salinity [28]. Salt and brine solutions are widely found in industry (e.g. offshore applications) and multi-parameter monitoring systems are therefore highly desirable for the determination of various key parameters such as oxygen concentration, proton concentration, and salinity.

In this paper, we report the use of microwire electrodes and chronoamperometry for measurement of concentration and diffusion coefficient data for protons and oxygen in

acidified brine (NaCl) solutions. Simultaneous quantification of both the concentration and diffusion coefficient parameters is performed by single-parameter fitting simulated chronoamperometric data employing the commercial software programme DigiElch. From the obtained oxygen concentration and diffusivity information the salinity can be approximated.

2. Experimental

2.1. Chemical Reagents

Potassium ferrocyanide ($K_4Fe(CN)_6$, > 99 %) was purchased from Fisher Scientific and used as received. Potassium chloride (KCl, > 99 %), sodium chloride (NaCl, > 99.5 %) and hydrochloric acid (HCl, stabilised at 1 M) were obtained from Sigma Aldrich UK. Solutions of NaCl/HCl ranging from 0.1 M to 4 M NaCl containing different concentrations of HCl were prepared using purified water with a resistivity of not less than 18 MΩ cm at 22 ºC (Millipore). Nitrogen gas (N_2) was purchased from BOC UK.

2.2. Instrumentation

Electrochemical experiments were carried out in a thermo-jacketed electrochemical cell connected to a water bath (Haake) maintained at 25 ± 0.5 ºC. Electrochemical measurements were performed using a microAutolab III potentiostat system (Eco Chemie, Netherlands). A standard three-electrode set-up was used using a KCl-saturated calomel reference (SCE) electrode, a Pt wire counter electrode, and a 25 μm diameter Pt microwire as the working electrode (see below). Digital simulation and data fitting was performed using the commercial software DigiElch 4.F selecting the semi-

infinite one-dimensional model with cylindrical geometry on a PC running Windows 7 32-Bit with an Intel Core i3 2.53 GHz processor and 4 GB RAM.

2.3. Procedure I.: Electrode Fabrication

A 25 μm diameter Pt wire (Advent UK) was laminated using commercial laminating plastic foil following a literature procedure [29]. A rectangle of approximately 18 cm × 2 cm was cut out, with a window of approximately 3 cm × 1 cm, where after thermal lamination (with a domestic iron) the platinum wire is exposed to the aqueous solution (see Figure 2). A piece of conducting copper tape (3M) was used to ensure electrical contact. The wire diameter needs to be confirmed by optical microscopy.

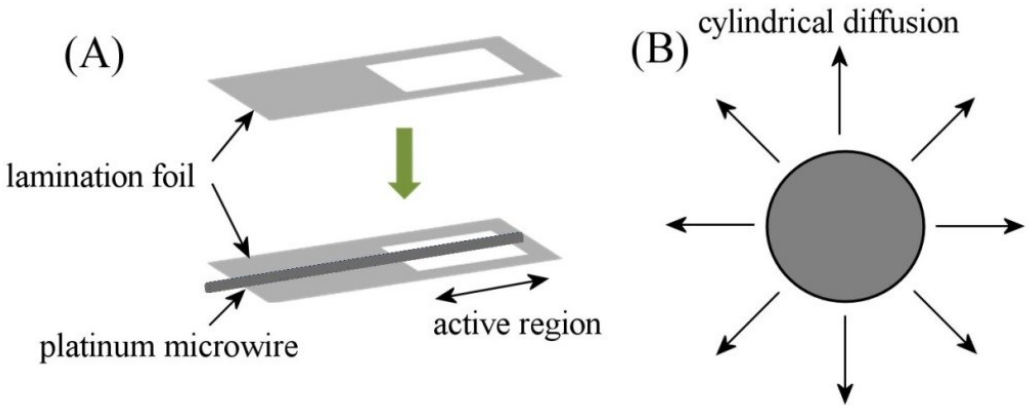

Figure 2. (A) Schematic of the fabrication process of the Pt microwire electrode. (B) Schematic drawing of the cylindrical diffusion field around the microwire.

2.4. Procedure II.: Microwire Chronoamperometry and Calibration

In order to calibrate the microwire length, chronoamperometry was performed for the one-electron oxidation of 2 mM ferrocyanide in 0.1 M KCl . Determination of the appropriate potential step parameters was first achieved by cyclic voltammetry (see

Figure 3A). Potential step transients were recorded by by stepping the potential from –0.10 V to 0.60 V vs. SCE and the current measured for 1 s using a sampling time of 2.5 ms (see Figure 3B). To avoid double-layer charging effects, the first 5 ms of data were discarded for the fitting procedure.

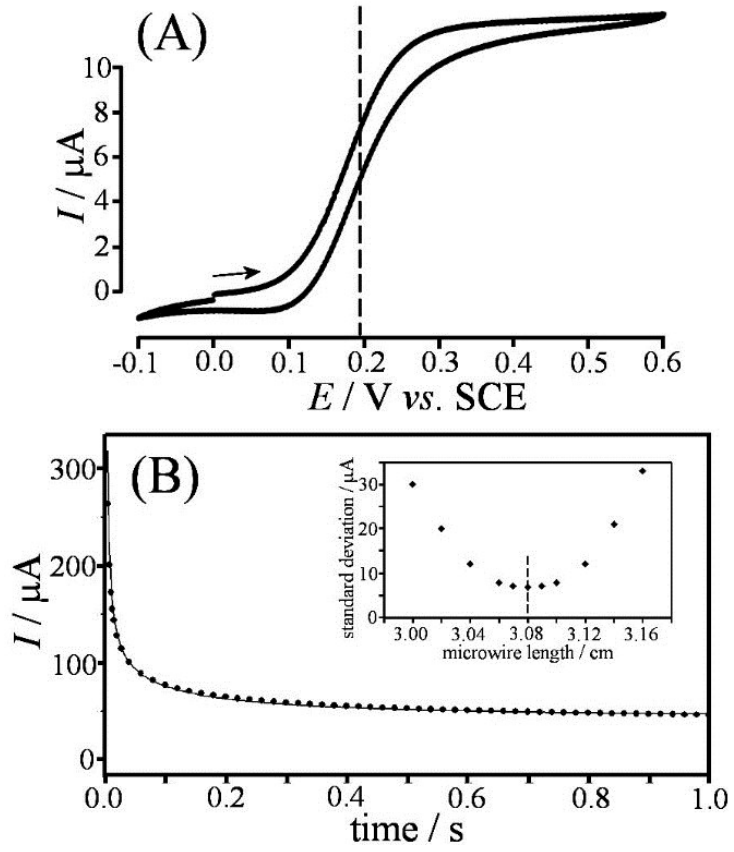

Figure 3. (A) Cyclic-voltammogram (scan rate 20 mV s^{-1}) for the oxidation of 2 mM potassium ferrocyanide in aqueous 0.1 M KCl at a 25 μm diameter Pt microwire electrode. (B) Chronoamperometric response (line) and simulation (dots) for the oxidation of 2 mM ferrocyanide. The inset shows the standard deviation for data fitting as a function of the microwire length, which is calibrated to 3.08 cm.

The calibration of the microwire length was achieved by digital simulation using the known concentration, 2 mM ferrocyanide, and the known diffusion coefficient under these conditions, of 0.65 × 10^{-9} m^2 s^{-1} at 25 ºC [30]. By systematically varying the electrode length parameter in the commercial DigiElch 4.F [19,20] software (Gamry

Instruments) and plotting the standard deviation (see Figure 3B inset) the microwire length was determined at 3.08 cm. For the determination of the concentration of oxygen or protons the calibrated length was employed and triplicate measurements were performed with standard error estimation based on the standard deviation.

3. Results and Discussion

3.1. Microwire Chronoamperometry I.: Proton Reduction in High Ionic Strength Media

Figure 4A shows voltammetric data for the reduction of 2 mM protons (equation 3) in 2.0 M NaCl at a 25 μm diameter platinum microwire electrode. The reversible potential is observed at -0.42 V vs. SCE with water reduction defining the potential window at -1.0 V vs. SCE.

$$H^+(aq) + e^- \rightarrow \frac{1}{2} H_2(aq) \qquad (3)$$

Chronoamperometry was performed by stepping the potential from 0.0 to -0.6 V vs. SCE (see Figure 4B). To simultaneously obtain the proton concentration and diffusion coefficient from the chronoamperometric data, the diffusion coefficient parameter in DigiElch was allowed to be iterated and optimised by the software whilst the proton concentration parameter was varied manually between 1 mM and 3 mM. The resulting parabolic standard deviation plot (see inset in Figure 4B) allows the concentration to be obtained. Proton concentrations and diffusion coefficients were determined in this way for a range of salinities and nominal proton concentrations of 2.0 mM and 0.5 mM (see

Figure 4C). The proton concentrations were successfully confirmed to be within +/- 5% of the nominal values whilst the diffusion coefficients measured in 0.1 M NaCl (8.1±0.9 $\times 10^{-9}$ m^2s^{-1} for 2 mM HCl and 7.8 ±0.9 $\times 10^{-9}$ m^2s^{-1} for 0.5 mM HCl) are in excellent agreement with the previous literature value of $D_{H+} = 7.8 \times 10^{-9}$ m^2s^{-1}, measured for a solution of 0.1 M KNO_3 [31].The proton diffusion coefficients were observed to decrease significantly with increasing solution salinity (reaching approximately half the above value at 4.0 M NaCl), which is attributed to the concomitant change in solution viscosity.

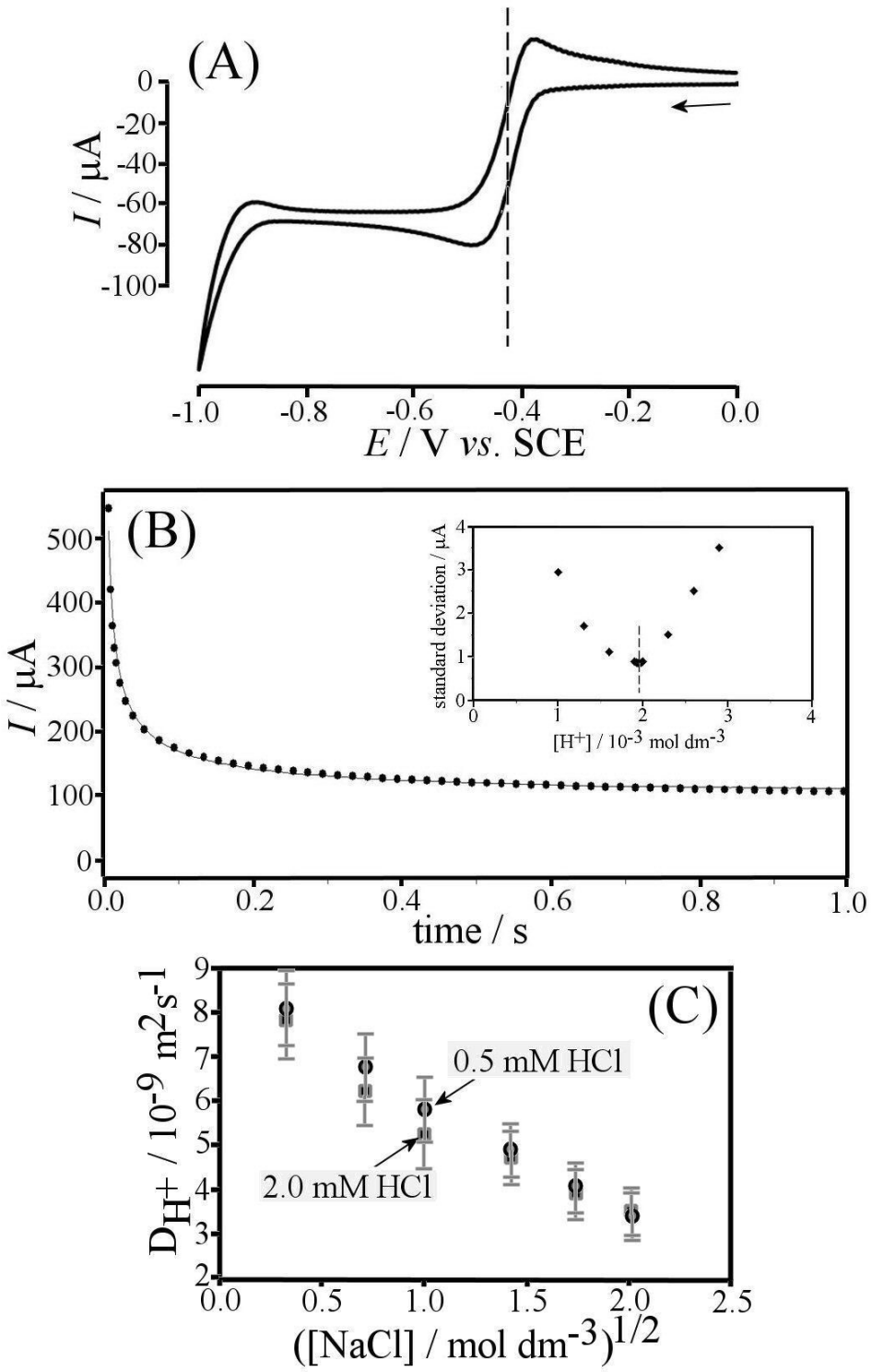

Figure 4. (A) Cyclic-voltammogram (scan rate of 50 mV s^{-1}) for the reduction of 2 mM protons in deaerated aqueous 2.0 M NaCl at a 25 μm diameter Pt microwire electrode. (B) Chronoamperometric data (potential step from 0.0 to -0.6 V vs. SCE) shown as line and the corresponding digital simulation data shown as dots. Inset: standard deviation plot for concentration optimisation. (C) Plot of the proton diffusion coefficients for 0.5 mM and for 2.0 mM protons versus square root of NaCl concentration (standard errors evaluated for triplicate measurements).

3.2. Microwire Chronoamperometry II.: Oxygen Reduction in High Ionic Strength Media

The reduction of oxygen to water (a four-electron process, equation 4) on platinum occurs at a potential more positive compared to that for proton reduction [32]. Figure 5A shows a typical cyclic voltammgram obtained for an ambient concentration of oxygen in the presence of 3 mM protons and in 4.0 M NaCl. The drawn-out shape of the voltammograms reveals overall slow (irreversible) electron transfer kinetics [33].

$$O_2(aq) + 4e^- + 4H^+(aq) \rightarrow 2H_2O(aq) \qquad (4)$$

A concentration of 3 mM protons was selected for oxygen reduction experiments to ensure a sufficient supply of protons and avoid further complications in electrode kinetics due to proton transport. Chronoamperometry was again performed (stepping from the potential 0.4 to -0.2 V vs. SCE, see Figure 5B) and the transient data analysed as above using the single parameter standard deviation approach (see inset Figure 5B). Both diffusion coefficient data and equilibrium oxygen concentration data are plotted in Figure 5C.

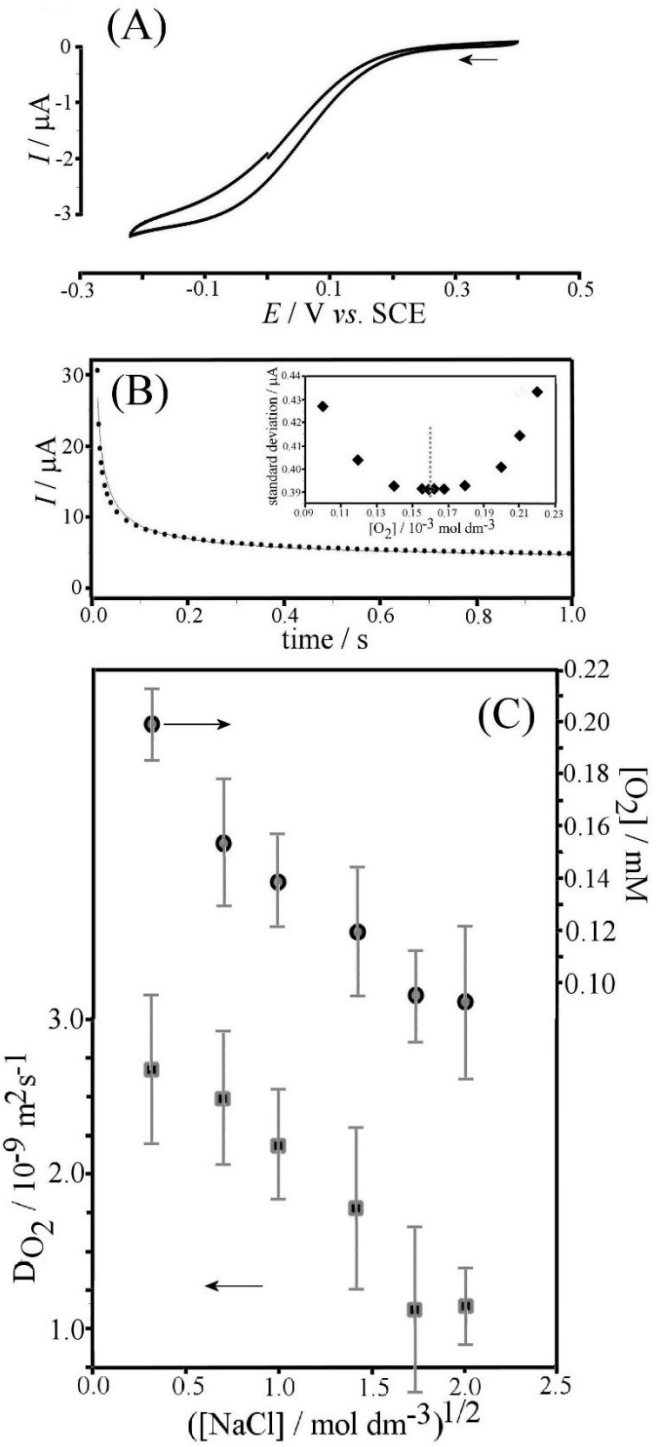

Figure 5. (A) Cyclic voltammogram (scan rate of 50 mV s^{-1}) for the reduction of ambient oxygen at a 25 μm diameter Pt microwire electrode in the presence of 3 mM protons in aqueous 4.0 M NaCl. (B) Chronoamperometry (potential step from +0.4 to -0.2 V vs. SCE). Inset showing the standard deviation optimisation to give the oxygen concentration. (C) Plot of the oxygen diffusion coefficient and the oxygen concentration as a function of square root of aqueous NaCl concentration (standard errors evaluated for triplicate measurements).

Unlike for protons, the dissolved oxygen concentration in NaCl solution varies with salinity due to the salting out effect. The equilibrium concentration values determined here are in agreement with literature data measured in, for example in KOH [34], although slightly lower than reported for seawater [35]. Error bars based on triplicate measurements appear to be relatively large, probably mainly due to variations in oxygen reduction kinetics, which notoriously result from changes in platinum surface condition but are assumed absent in the transient data analysis. Given such phenomena will affect the early data points in particular, the chronoamperometric approach is expected to be sensitive, although further improvements are possible. The diffusion coefficeint data for oxygen are slightly higher than those in literature reports (for pure water $D_{O2} = 2 \times 10^{-9}$ m^2s^{-1} at 25 ^oC [36]) indicative of a remaining systematic error in the analysis. Diffusion coefficeint data reveal a very similar trend with salinity compared to that observed for proton diffusion coefficients. These results are consistent with a viscosity effect and confirm Walden's law [37].

3.3. Microwire Chronoamperometry III.: Simultaneous Proton, Oxygen, and Salinity Determination

The fact that proton and oxygen reduction occur at different potentials and their diffusion coefficients depend on salinity enables application of this methodology to simultaneous multi-parameter electroanalytical problems. This versatility was demonstrated using a solution containing 3 mM protons in 1.0 M NaCl. The cyclic voltammogram in Figure 6A shows the distinct responses for the reduction of oxygen at +0.1 V vs. SCE and the reduction of protons at -0.4 V vs. SCE. By performing a double-step chronoamperomemtric experiment, firstly from +0.75 to -0.25 V vs. SCE

(for oxygen determination) and then from -0.25 to -0.90 V vs. SCE (for proton determination), the diffusion coefficient and concentration of both of these species can be estimated within a single double-step experiment. From the chronoamperometric data fitting process (see Figure 6B) the oxygen concentration was determined to be 124 μM with a diffusion coefficeint of $D_{O2} = 2.2 \times 10^{-9}$ m^2s^{-1}. Comparison with Figure 5C indicates that both values agree well with a salinity of 1 M NaCl. Next the fitting process was applied to proton reduction (without accounting for the simultaneous oxygen reduction, see Figure 6C), for which the proton concentration was determined to be 2.49 mM and $D_{H+} = 7.25 \times 10^{-9}$ m^2s^{-1}. Since protons are also consumed during the underlying oxygen reduction step we know that approximately 4 × 0.124 mM = 0.5 mM protons are excluded from this measurement. Hence the total calculated proton concentration is adjusted to 2.99 mM in excellent agreement with the nominal value of 3.0 mM.

The full simulation of proton reduction with underlying oxygen reduction is possible with the concentration and diffusion coefficeint for oxygen known. Based on full digital simulation with the 4-electron reduction of oxygen and the coresponding fast consumption of four protons directly generated values of $c_{H+} = 3.0$ mM and $D_{H+} = 7.27 \times 10^{-9}$ m^2s^{-1} (see Figure 6D) in excellent agreement with the previous result.

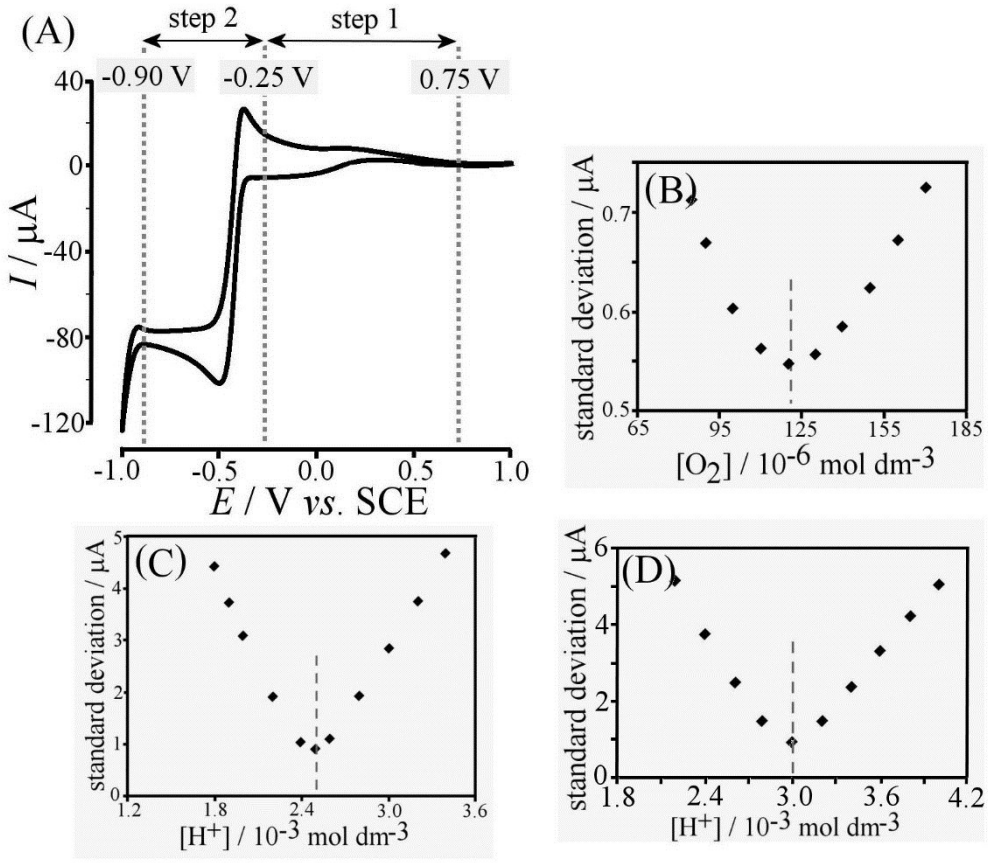

Figure 6. (A) Cyclic voltammogram (scan rate of 50 mV s^{-1}) for the reduction of ambient oxygen at a 25 µm diameter Pt microwire electrode in the presence of 3 mM protons in aqueous 1.0 M NaCl. (B) Data for minimisation of error for chronoamperometry (potential step from 0.75 to -0.25 V vs. SCE) to give the oxygen concentration 0.12 mM. (C) Data for minimisation of error for chronoamperometry (potential step from -0.25 to -0.90 V vs. SCE) to give the proton concentration 2.5 mM. (D) As in C but with oxygen reduction accounted for to give a proton concentration of 3.0 mM (see text).

From these results it is clear that the double-step experiment coupled to numerical simulation and fitting analysis allows simultaneous determination of oxygen concentration, oxygen diffusion coefficeint, proton concentration, proton diffusion coefficeint, and salinity. Digital simulation allows parallel processes and loss of protons to be accounted for. In the case of an unknown sample or a monitoring problem where a solution of unknown oxygen content, proton concentration, and salinity is present,

this methodology could be employed directly (with a calibrated electrode and automated data fitting) and *in situ*.

4. Summary and Conclusion

A microwire-based method has been developed for multi-parameter determination of concentration and diffusivity information in saline solutions. The microwire method is relatively robust (not affected by viscosity effects and less sensitive to imperfections in mounting in comparison to microdiscs, which are extremely sensitive to salt solution penetration into cracks between platinum and glass) and when coupled to numerical simulation tools (here the commercial DigiElch package) extremely powerful.

The methodology introduced here allows both the concentration of oxygen and the concentration of protons to be determined simultaneously (first potential step for oxygen concentration and diffusion coefficient; second potential step for proton concentration and diffusion coefficient) in mixed solutions containing high levels of NaCl. The oxygen concentration and diffusivity information can in turn be used to estimate the salinity of the electrolyte solution, although further work may be required to improve experimental precision. In future other parameters (including kinetic rate data and co-reactant information) could be extracted and the analysis process could be further automated for example for online monitoring purposes.

Acknowledgements

J.W. and A.J.W acknowledge the financial support of the UK National Measurement System.

References

[1] K. Aoki, *Electroanalysis*, **1993**, *5*, 627-639.

[2] L.K. Bieniasz, *Electrochim. Acta*, **2011**, *56*, 6982-6988.

[3] D. Britz, O. Osterby, J. Strutwolf, *Electrochim. Acta*, **2010**, *55*, 5629-5635.

[4] K. Aoki, K. Honda, K. Tokuda, H. Matsuda, *J. Electroanal. Chem.*, **1985**, *182*, 267-279.

[5] L. Lu, G. Chee, K. Yamada, S. Jun, *Biosens. Bioelectronics*, **2013**, *42*, 492-495.

[6] M.L. Agui, A.J. Reviejo, P. Yanezsedeno, J.M. Pingarron, *Anal. Chem.*, **1995**, *67*, 2195-2200.

[7] M. Somasundrum, K. Aoki, *J. Electroanal. Chem.*, **2002**, *530*, 40-46.

[8] M.J. Nuwer, J. Osteryoung, *Anal. Chem.*, **1989**, *61*, 1954-1959.

[9] G. Billon, C.M.G. van den Berg, *Electroanalysis,* **2004**, *16*, 1583-1591.

[10] Z.S. Bi, P. Salaun, C.M.G. van den Berg, *Marine Chem.*, **2013**, *151*, 1-12.

[11] V. Aumond, M. Waeles, P. Salaun, K. Gibbon-Walsh, C.M.G. van den Berg, P.M. Sarradin, R.D. Riso, *Anal. Chim. Acta*, **2012**, *753*, 42-47.

[12] J. Ellison, C. Batchelor-McAuley, K. Tschulik, R.G. Compton, *Sens. Actuators B-Chem.*, **2014**, *200*, 47-52.

[13] P. Gründler, A. Kirbs, L. Dunsch, *ChemPhysChem*, **2009**, *10*, 1722-1746.

[14] A. Beckmann, B.A. Coles, R.G. Compton, P. Gründler, F. Marken, A. Neudeck, *J. Phys. Chem. B*, **2000**, *104*, 764-769.

[15] M.M. Murphy, J.J. Odea, J. Osteryoung, *Anal. Chem.*, **1991**, *63*, 2743-2750.

[16] L.K. Bieniasz, *J. Electroanal. Chem.*, **2011**, *662*, 371-378.

[17] A.J. Bard, L.R. Faulkner, *Electrochemical Methods*, John Wiley, New York, 2001, p. 163.

[18] A. Szabo, D.K. Cope, D.E. Tallman, P.M. Kovach, R.M. Wightman, *J. Electroanal. Chem.*, **1987**, *217*, 417-423.

[19] J. Windhager, M. Rudolph, S. Bräutigam, H. Gorls, W. Weigand, *European J. Inorg. Chem*., **2007**, *18*, 2748-2760.

[20] M. Rudolph, *J. Comput. Chem.*, **2005**, *26*, 1193–1204, and literature cited therein.

[21] A.J. Bard, L.R. Faulkner, *Electrochemical Methods*, John Wiley, New York, 2001, p. 163.

[22] C. Amatore in *Physical Electrochemistry*, I. Rubinstein (ed.), Marcel Dekker, New York, 1995, p. 131.

[23] L.H.J. Xiong, L. Aldous, M.C. Henstridge, R.G. Compton, *Anal. Methods*, **2012**, *4*, 371-376.

[24] O.V. Klymenko, R.G. Evans, C. Hardacre, I.B. Svir, R.G. Compton, *J. Electroanal. Chem.*, **2004**, *571*, 211-221.

[25] M. Forbes, S. Lynn, *AIChE J.*, **1975**, *21*, 763-769.

[26] L.K. Ju, C.S. Ho, *Biotechnol. Bioengineering,* **1985**, *27*, 1495-1499.

[27] A.J. Vanstroe, L.J.J. Janssen, *Anal. Chim. Acta*, **1993**, *279*, 213-219.

[28] F.J. Millero, F. Huang, A.L. Laferiere, *Marine Chem*., **2002**, *78*, 217-230.

[29] A. Neudeck, L. Kress, *J. Electroanal. Chem.*, **1997**, *437*, 141-156.

[30] R.N. Adams, *Electrochemistry at solid electrodes*, Marcel Dekker, New York, 1969, p. 219.

[31] J.V. Macpherson, P.R. Unwin, *Anal. Chem.*, **1997**, *69*, 2063-2069.

[32] C.H. Chen, K.E. Meadows, A. Cuharuc, S.C.S. Lai, P.R. Unwin, *Phys. Chem. Chem. Phys.*, **2014**, *16*, 18545-18552.

[33] V. Stamenkovic, N.M. Markovic, P.N. Ross, *J. Electroanal. Chem.*, **2001**, *500*, 44-51.

[34] L. Nei, F. Marken, Q. Hong, R.G. Compton, *J. Electrochem. Soc*., **1997**, *144*, 3019-3026.

[35] H.E. Garcia, L.I. Gordon, *Limnology Oceanography*, **1992**, *37*, 1307–1312.

[36] K.E. Gubbins, R.D. Walker, *J. Electrochem. Soc.*, **1965**, *112*, 469-470.

[37] P.W. Atkins, *Physical Chemistry*, Oxford University Press, Oxford, 1995, p. 850.